INFLUENCE OF VELOCITY GRADIENT AND WALL PROXIMITY ON THE READINGS OF A PITOT TUBE IN MEASUREMENT OF SURFACE FRICTION AND VELOCITY DISTRIBUTION IN A TURBULENT BOUNDARY LAYER

E. U. Repik, V. K. Kuzenkov, and N. P. Mikhailova

UDC 532.574

The authors present results of an experimental investigation of the correlations and readings of a Pitot tube in measuring velocity in a turbulent boundary layer. A new calibration relation is proposed for measuring surface friction.

The use of a total head or Pitot tube to measure the velocity in a boundary layer in the close proximity of a washed surface (a wall) requires corrections for the readings, because:

a) one cannot use ideal fluid theory to interpret the total pressure measured by the tube under low Reynolds number conditions in close proximity to a wall (influence of viscosity);

b) the transverse velocity gradient in the boundary layer and the wall proximity influences the Pitot tube readings.

The influence of viscosity on the readings of Pitot tubes of different geometrical form has been rather fully investigated in [1, 2]. Regarding the influence of velocity gradient and wall proximity, the available theoretical solutions in [3, 4] and the several test data [5-7] on this matter are very contradictory and show poor interagreement, which makes it difficult to use them in practice.

Below we present the results of a systematic experimental investigation of the combined influence of velocity gradient and wall proximity on the readings of a Pitot tube with a curved aperture, results of which both improve the existing information on this topic and lend themselves to practical application to the measurement of surface friction and velocity distribution in a turbulent boundary layer.

1. A deviation of the measured velocity profile in a boundary layer from the true profile may be associated either with an error in determining the distance of the Pitot tube from the wall, or with an error in determining the velocity itself. Investigators usually prefer the second cause. In this case the error is determined by direct comparison of the velocities measured by the tube u_{meas} with the true velocities u_{true}, where u_{meas} is determined by using the Bernouilli equation ($P_0 = P_{st} + \rho u^2/2$).

Because we have no accurate theoretical solutions, the true velocity distribution in the turbulent boundary layer is determined from experiment, as follows.

One can postulate that the error due to the influence of velocity gradient and wall proximity on the Pitot tube readings will be less, the smaller is the diameter of the tube D, and as $D \to 0$ the measured velocity approaches the true value. In this way, the value of u_{true} in the boundary layer in our tests was determined by extrapolation to the case $D = 0$ the velocity values measured using circular Pitot tubes with various inlet diameters, mounted at fixed distances from the wall. The straight lines (Fig. 1a) describing the relation $u = f(D)$, were drawn through the test points using the least-squares method, and to the measured velocities we first applied corrections to account for possible deviation of the tube pressure coefficient $c_p = (P_0 - P_{st})/(\rho u^2/2)$ from 1 (the influence of viscosity). The values of c_p describing the degree of correlation of velocity and pressure were determined from the empirical formula [1]

$$c_p = \mathrm{Re}'_D [1.07\ \mathrm{Re}'_D - 3.7]^{-1},$$

Translated from Inzhenerno-Fizicheskii Zhurnal, Vol. 48, No. 6, pp. 895-904, June, 1985. Original article submitted March 21, 1984.

0022-0841/85/4806-0642$09.50

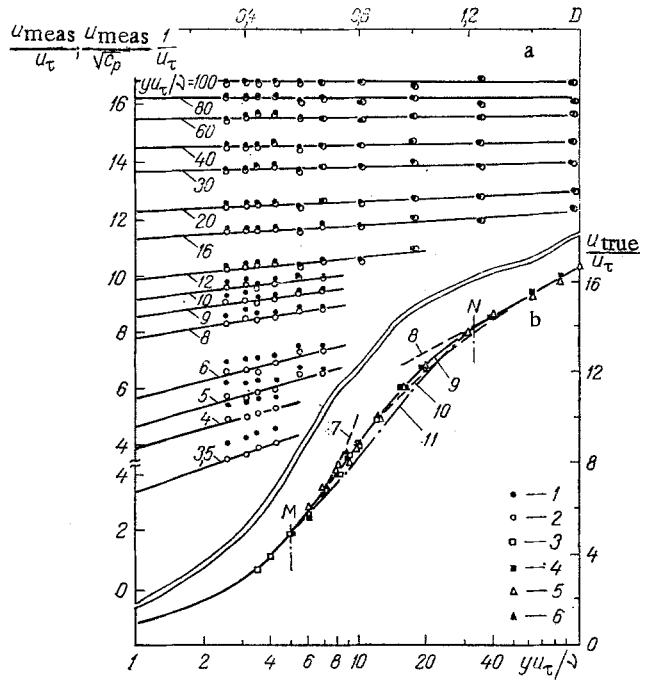

Fig. 1. Pitot tube readings as a function of tube diameter at different Re_y values (a), and the true velocity distribution in the transition zone of a turbulent boundary layer (b) (D in mm): 1) without correction for viscosity (u_{meas}/u_τ); 2) with correction for viscosity ($u_{meas}/\sqrt{c_p}$)/u_τ; 3) u_τ = 0.23 m/sec (Re** = 590); 4) u_τ = 0.31 m/sec (Re** = 977); 5) u_τ = 0.39 m/sec (Re** = 1232); 6) u_τ = 0.51 m/sec (Re** = 1613); 7) from Eq. (3); 8) from Eq. (1); 9) from Eq. (2); 10) from Eq. (4); 11) from Eq. (5).

where

$$\mathrm{Re}'_D = uD/(2\nu).$$

The measurements were made in a turbulent boundary layer on a flat plate at Reynolds numbers based on the momentum loss thickness Re** = $u_\infty\delta^{**}/\nu$, equal to 590, 977, 1232, and 1613. In the tests we used Pitot tubes with outside diameters of 0.332, 0.400, 0.442, 0.506, 0.592, 0.674, 0.810, 1.000, 1.240, and 1.574 mm, and the ratio of the tube inside-to-outside diameter was constant and equal to 0.6.

As can be seen from Fig. 1a at large distances from the wall, when the Reynolds number $Re_y = yu_\tau/\nu$, based on the friction velocity u_τ and the distance y from the wall greater than 60, the Pitot tube readings are practically independent of the diameter. In this case, because the velocity gradient in the boundary layer is small, it does not influence the tube readings. There is also no viscosity influence, since the tube pressure coefficient c_p for $Re_y > 60$ approaches 1, and the flow velocity can be determined by use of the Bernouilli equation.

As one approaches the wall, when the velocity gradient in the boundary layer begins to increase appreciably ($Re_y < 20$), the measured velocities become less, the smaller the tube diameter. The tube pressure coefficient becomes appreciably larger than 1 and, therefore, the velocities as corrected for viscosity ($u_{meas}/\sqrt{c_p}$)/u_τ fall below the uncorrected values u_{meas}/u_τ.

Here it should be noted that the Pitot tube diameters were chosen so that the measurements could be conducted in the transition zone of the turbulent boundary layer, where the velocity distribution law has been least studied.

The true velocity profile in the turbulent boundary layer in dimensionless coordinates $u/u_\tau = f(yu_\tau/\nu)$, obtained from these experiments, can be described by the following relations (Fig. 1b):

in the turbulent core

$$u/u_\tau = A \lg (yu_\tau/\nu) + B, \quad A = 5.63 \text{ and } B = 5.4; \tag{1}$$

in the transition zone

$$u/u_\tau = -7.44 (\lg yu_\tau/\nu)^3 + 21.0 (\lg yu_\tau/\nu)^2 - 6.96 \lg yu_\tau/\nu + 2.14. \tag{2}$$

In the viscous sublayer region ($yu_\tau/\nu < 5$) the test points agree with the linear law

$$u/u_\tau = yu_\tau/\nu. \tag{3}$$

The constant coefficients in Eq. (2) were chosen from the condition of best agreement with experiment in a continuous distribution of velocity and its first derivative at the points M($yu_\tau/\nu = 5$, $u/u_\tau = 5$) and N($yu_\tau/\nu = 33$, $u/u_\tau = 13.95$), corresponding to matching Eq. (2) with the linear relation Eq. (3) and the logarithmic law of Eq. (1).

In determining the friction velocity $u_\tau = \sqrt{\tau_w/\rho}$ the value of the shear stress τ_w was determined from the true velocity values in the close proximity of the wall, in the viscous sublayer region, using the relation

$$\tau_w = \mu \left(\frac{\partial u}{\partial y}\right)_w = \mu \frac{u_{\text{true}}}{y}.$$

A comparison of the shear stress values thus obtained with τ_w as directly measured by a weighting method using a floating element has shown that the two agree to within the scatter of the test points, which does not exceed ±4%.

Figure 1b also shows for comparison the velocity profiles in the transition zone of the turbulent boundary layer, as calculated according to Spalding [8]

$$yu_\tau/\nu = u/u_\tau + e^{-C}\left\{e^{ku/u_\tau} - \left[1 + ku/u_\tau + \frac{(ku/u_\tau)^2}{2!} + \frac{(ku/u_\tau)^3}{3!} + \frac{(ku/u_\tau)^4}{4!}\right]\right\} \tag{4}$$

and, according to Reichardt [9]:

$$u/u_\tau = \frac{1}{k} \ln (1 + kyu_\tau/\nu) + \left(B - \frac{1}{k} \ln k\right)\{1 - e^{-(yu_\tau/\nu)/11} - [(yu_\tau/\nu)/11] e^{-0.33yu_\tau/\nu}\}, \tag{5}$$

where $k = (A/\ln 10)^{-1} = 0.409$, $C = (B/A)/\ln 10 = 2.208$, and here the constant coefficients in Eqs. (4) and (5) were chosen, taking Eq. (1) into account, to obtain the best agreement between theory and experiment.

2. We shall consider the case when the Pitot tube is positioned at the wall.

Figure 2 shows the ratio of the measured to true velocity values as a function of the Reynolds number $\text{Re}_D = Du_\tau/\nu$. Here u_{true} corresponds to the axis of the Pitot tube. It can be seen that for $\text{Re}_D < 50$ the ratio $\vartheta_0 = u_{\text{meas}}/u_{\text{true}}$ is greater than 1 (solid line). Introducing a correction to the measured velocity values for the influence of flow viscosity $\vartheta_1 = (u_{\text{meas}}/\sqrt{c_p})/u_{\text{true}}$ for $\text{Re}_D < 10$ appreciably reduces the ratio of the velocities (see the broken line). For $\text{Re}_D < 5$ the broken line results in a constant value equal to 1.32. If we consider the deviation of the velocity profile measured by the Pitot tube from the true velocity profile as an error in determining the distance of the tube from the wall, i.e., we link this deviation to displacement of the effective center of the Pitot tube from its geometrical axis (ε), then the value $\vartheta_1 = 1.32$ will correspond to $\varepsilon/D = 0.16$.

Indeed, if the tube is completely immersed in the viscous sublayer, where the velocity distribution is linear, then we have (see Fig. 5a):

$$\frac{u_{\text{meas}} - u_1}{u_{\text{true}} - u_1} = \frac{\varepsilon + D/2}{D/2}, \text{ where } u_{\text{true}} = u_c$$

or (allowing for viscosity):

$$\vartheta_1 = 1 + 2\alpha\varepsilon/D,$$

where $\alpha = (u_2 - u_1)/(2u_c)$. In the case when the tube is positioned at the wall ($u_1 = 0$), the value of α is 1.

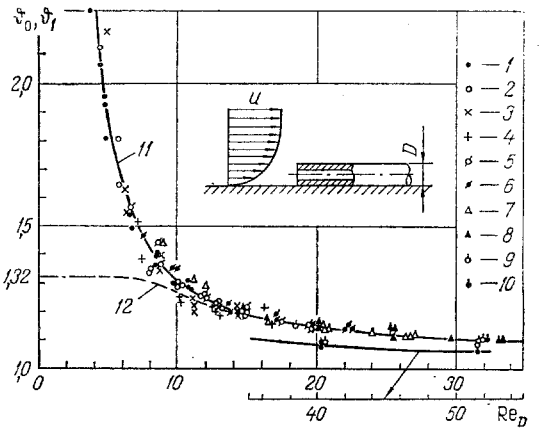

Fig. 2

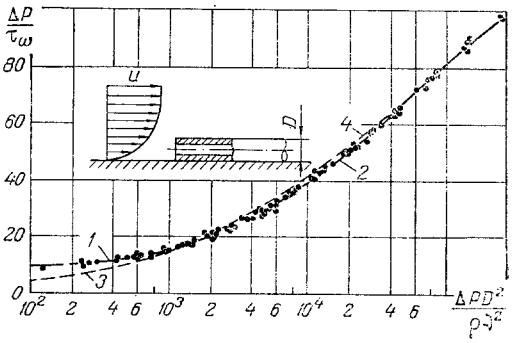

Fig. 3

Fig. 2. Readings of the Pitot tube positioned at the wall as a function of u_τ/ν = (11.1-32.7)•10^3 m^{-1}: 1) D = 0.332 mm; 2) 0.400; 3) 0.442; 4) 0.506; 5) 0.592; 6) 0.674; 7) 0.810; 8) 1.000; 9) 1.240; 10) 1.574; 11) without correction for viscosity ϑ_0; 12) with correction for viscosity, ϑ_1.

Fig. 3. Calibration relations for the indirect method of measuring surface friction with the aid of a circular Pitot tube positioned at the wall: 1, 2) Eqs. (8) and (9), respectively; 3, 4) calculated from the Patel relations, Eqs. (10) and (11).

From the test data shown in Fig. 2 we can obtain a calibration relation for the indirect method of measuring surface friction with the aid of a Pitot tube, known as the Preston method [10]. The Preston method is based on using the universal properties of the "law of the wall" in the boundary layer

$$u/u_\tau = f(yu_\tau/\nu),$$

which can easily be transformed to the form

$$\frac{\rho D^2 \tau_w}{\mu^2} = \varphi\left(\frac{\rho D^2 \Delta P}{\mu^2}\right) \tag{6}$$

or to the more preferable form

$$\frac{\Delta P}{\tau_w} = F\left(\frac{\Delta P D^2}{\rho\nu^2}\right). \tag{7}$$

It follows from Eqs. (6) and (7) that τ_w can be found if we know the physical properties of the liquid (ρ, μ, ν) and the value $\Delta P = P_0 - P_{st}$ measured with the aid of a Pitot tube positioned directly at the wall and a static pressure drain aperture.

The functional dependence of Eq. (7) obtained in these tests can be described by the following relations (Fig. 3):

$$\frac{\Delta P}{\tau_w} = 0.031\left(\lg\frac{\Delta P D^2}{\rho\nu^2}\right)^5 + 8{,}29 \tag{8}$$

for $\Delta PD^2/\rho\nu^2 \leq 6.5\cdot10^3$ and

$$\frac{\Delta P}{\tau_w} = -5.472\left(\lg\frac{\Delta P D^2}{\rho\nu^2}\right)^3 + 78.17\left(\lg\frac{\Delta P D^2}{\rho\nu^2}\right)^2 - 327{,}9\lg\frac{\Delta P D^2}{\rho\nu^2} + 450.4 \tag{9}$$

for $6.5\cdot10^3 < (\Delta PD^2/\rho\nu^2) < 2.5\cdot10^5$.

For comparison, Fig. 3 shows also the calibration relations of Patel [11] which he obtained in the coordinates of Eq. (6) and which have the form

$$y^* = 0{,}5x^* + 0{,}037 \quad \text{for} \quad y^* < 1{,}5 \left(\frac{\Delta P D^2}{\rho\nu^2} < 3{,}2\cdot10^3\right), \tag{10}$$

$$y^* = 0.8287 - 0.1381x^* + 0.1437x^{*^2} - 0.006x^{*^3} \tag{11}$$

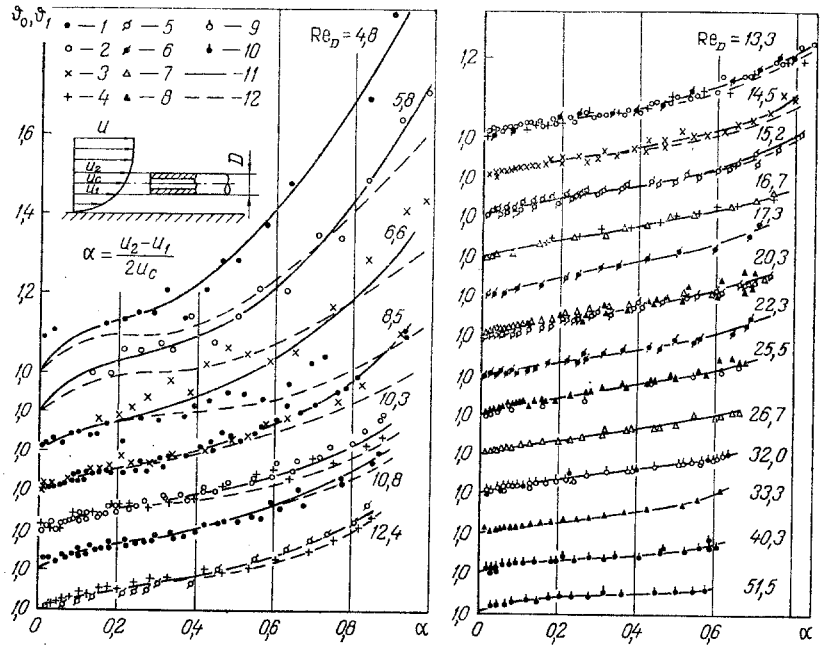

Fig. 4. Readings of the Pitot tube during a traverse across a turbulent boundary layer as a function of the transverse velocity gradient parameter α and the Reynolds number Re$_D$: 1) D = 0.332 mm; 2) 0.400; 3) 0.442; 4) 0.506; 5) 0.592; 6) 0.674; 7) 0.810; 8) 1.000; 9) 1.240; 10) 1.574; 11) without correction for viscosity ϑ_0; 12) with correction for the viscosity ϑ_1.

$$\text{for} \quad 1.5 < y^* < 3.5 \left(3.2 \cdot 10^3 < \frac{\Delta P D^2}{\rho \nu^2} < 1.6 \cdot 10^6 \right), \tag{11}$$

where

$$x^* = \lg \left(\frac{\Delta P D^2}{4 \rho \nu^2} \right) \text{and } y^* = \lg \left(\frac{\tau_w D^2}{4 \rho \nu^2} \right).$$

It can be seen that at values of the parameter $\Delta PD^2/(\rho\nu)^2 < 1000$ the curve calculated from the Patel relations transformed to the form of Eq. (7), falls noticeably below the calibration curves of Eqs. (8)-(9) obtained in these tests. However, for $\Delta PD^2/(\rho\nu)^2 > 1000$ the agreement between the calibration relations of Eqs. (8)-(9) and the Patel relations can be considered satisfactory.

3. Figure 4 shows the test data in the case when the Pitot tube is traversed across the boundary layer.

Here $\alpha = 0$ when the tube goes completely outside the boundary layer, and $\alpha = 1$ when the tube is positioned at the wall and is completely immersed in the viscous sublayer with its linear velocity distribution law. And if the tube lies in the boundary layer, but goes outside the viscous sublayer, then, regardless of whether it is positioned at the wall or at some distance from the wall, the values of α will always be less than 1, $0 < \alpha < 1$. For $yu_\tau/\nu \geq 60$, when the Pitot tube readings become practically independent of the tube diameter (see Fig. 1a) the values of α are close to zero. For example, for $yu_\tau/\nu = 80$ the value of α does not exceed 0.04. The minimum value of α for a Pitot tube positioned at the wall is 0.5 and corresponds to the case when the tube radius is greater than the boundary-layer thickness ($u_2 = u_c$ and $u_1 = 0$). It should also be mentioned that the last points on all the curves of Fig. 4 ($\alpha = 0.6$-1.0) correspond to the case when the Pitot tube is at the wall.

The influence of viscosity on the tube readings appears noticeably for $Du_\tau/\nu < 10$ and disappears completely for $Du_\tau/\nu > 16$.

To illustrate the influence of the tube dimensions on its readings as a function of the boundary-layer parameters, Fig. 5a shows solid curves smoothed from the test points, obtained from Figs. 2 and 4. The figure shows the theoretical solutions of Hall [3] and Lighthill [4], in which the flow over a Pitot tube with a circular entrance aperture and with a

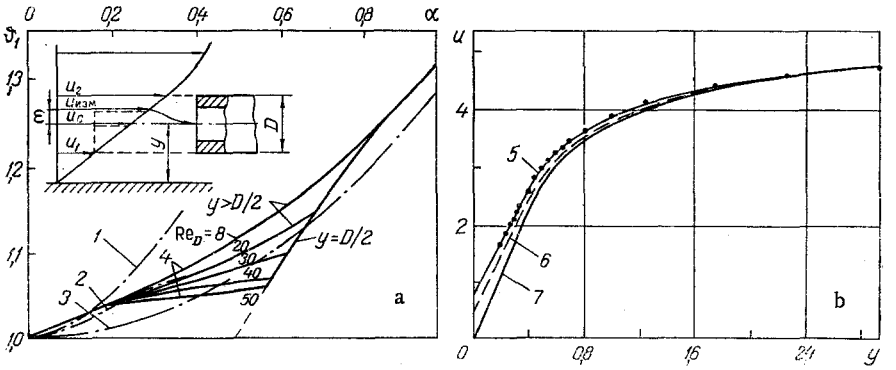

Fig. 5. Summary graph of corrections to the measured velocities in the turbulent boundary layer as a function of the transverse velocity gradient parameter α and the Reynolds number Re_D (a), and an example of determining the true velocity distribution in the turbulent boundary layer from the measured velocity distribution by a method of successive approximations (b) (u is in m/sec, y is in mm): 1) theory of Hall [3]; 2) theory of Lighthill [4]; 3) calculation according to Chue [13]; 4) present tests; 5) measured velocity distribution; 6) first approximation; 7) true velocity distribution.

straight lip is represented as flow over a sphere positioned far from a solid boundary (the wall), and here, in the first case, the vorticity field was considered in the longitudinal plane of symmetry of a sphere mounted in a skew flow and, in the second case, three-dimensional flow over a sphere was considered.

Both these theories indicate the same tendency for the variation of ϑ_1 as a function of α. However, numerically they do not agree between themselves and with the present test data in the boundary layer.

Analysis shows that the divergence between the measured and the true values of velocity in the boundary layer, or the displacement of the effective center of the Pitot tube, arises from the fact that:

a) when a Pitot tube is washed by a flow with a transverse velocity gradient one observes a deviation of the stream lines toward lower velocities, leading to an increase of the velocity values measured by the tube;

b) since the total pressure measured by the tube is proportional to the square of velocity, the velocity head averaged over the area of the tube entrance aperture, in the presence of a velocity gradient over the height of the aperture will not correspond to the geometric center of the tube, but to a certain effective center displaced toward higher velocities.

Estimates show that the latter fact leads to displacement of the effective tube center by an amount which is an order of magnitude less than the total displacement due to both effects [12]. In fact, for a Pitot tube of diameter D and an infinitely thin wall we have:

$$(P_0 - P_{st})\,\pi\,(D/2)^2 = \int_S \rho u^2/2 ds.$$

Assuming a linear distribution of velocity with height over the tube entrance aperture

$$u = u_{true}(1 + 2\alpha y'/D),$$

and also taking into account that $P_0 - P_{st} = \rho u^2_{meas}/2$, where $u_{meas} = u_{true}(1 + 2\alpha\varepsilon/D)$, we obtain

$$(\rho u^2_{true}/2)\,(1 + 2\alpha\varepsilon/D)^2\,\pi\,(D/2)^2 = (\rho u^2_{true}/2)\,(1 + \alpha^2/4)\,\pi\,(D/2)^2$$

or

$$16\alpha\,(\varepsilon/D)^2 + 16\varepsilon/D - \alpha = 0. \qquad (12)$$

It follows from Eq. (12) that if, for example, the Pitot tube is positioned in the boundary layer far from the wall with $\alpha = 0.2$, then the relative displacement of its effective center will be $\varepsilon/D = 0.012$ ($\vartheta_0 = 1.005$), and in the case when the tube is positioned at the wall and is completely immersed in the viscous sublayer ($\alpha = 1$), we obtain $\varepsilon/D = 0.059$ ($\vartheta_0 = 1.118$). For a tube with a finite wall thickness for $d/D = 0.6$ (where d is the tube inside diameter) we have: $(\varepsilon/D)(d/D) = 0.007$ for $\alpha = 0.2$ and $(\varepsilon/D)(d/D) = 0.035$ for $\alpha = 1$.

Thus, the main contribution to the displacement of the effective center of the Pitot tube relative to its geometric axis comes from deviation of the stream lines due to the presence of a velocity gradient in the boundary layer, and this leads to an appreciable divergence between the measured and the true velocity values.

Here it should be borne in mind that if the Pitot tube is positioned in the immediate proximity of the wall, then the wall begins to influence the nature of the flow over the tube, i.e., the degree of deviation of the stream lines and the nature of this deviation.

The curves shown in Fig. 5a, which describe values of ϑ_1 as a function of α for various values of Reynolds numbers Re_D, can be approximated by the following approximation formulas:

for the case when the Pitot tube is traversed across the boundary layer:

$$\vartheta_1 = 1 + 0.195\alpha, \quad 0 \leqslant \alpha \leqslant 0.2 \tag{13}$$

and

$$\vartheta_1 = 1.039 + a(\alpha - 0.2)^b, \quad 0.2 < \alpha \leqslant \alpha_{max}, \tag{14}$$

where

$$a = 0.469 - 1.3 \cdot 10^{-2} Du_\tau/\nu + 8.72 \cdot 10^{-5} (Du_\tau/\nu)^2,$$
$$b = 1.28 + 2.7 \cdot 10^{-4} Du_\tau/\nu - 2.36 \cdot 10^{-4} (Du_\tau/\nu)^2,$$

and for the case when the Pitot tube is located at the wall:

$$\vartheta_1 = 0.525 + 1.132\alpha - 0.338\alpha^2. \tag{15}$$

The values of α_{max} for the curves (Fig. 5a) calculated from Eqs. (14) can be found from the condition that the right-hand sides of Eqs. (14) and (15) be equal.

Equations (13)-(15) allow us to determine the true velocity distribution in a turbulent boundary layer from the velocity distribution measured with a Pitot tube. The values of α in Eqs. (13)-(14) are determined by successive approximations; here in the initial and first approximations in the case when the tube is positioned at the wall the value u_1 is found graphically (Fig. 5b) as the point of intersection with the axis of ordinates extrapolated to $y = 0$ by a straight line describing the current velocity distribution near the wall. From the current velocity distribution we also determine the values u_c and u_2.

Calculations show that the iterative sequence rapidly converges, and here in the last approximation the value u_1 for a tube located at the wall becomes equal to zero within the limits of the required accuracy.

NOTATION

u_{meas}, velocity measured by a Pitot tube using the Bernoulli equation; u_{true}, true velocity; $\vartheta_0 = u_{meas}/u_{true}$, ratio of the measured velocity to the true; $\vartheta_1 = (u_{meas}/\sqrt{c_p})/u_{true}$, ratio of the measured velocity with viscosity correction to the true velocity; c_p, Pitot tube pressure coefficient; P_o, total pressure; P_{st}, static pressure; ΔP, pressure drop; $u_\tau = \sqrt{\tau_w/\rho}$, friction velocity; τ_w, shear stress at the wall; ρ, ν, μ, density and kinematic and dynamic viscosity of the flow; $Re^{**} = u_\infty \delta^{**}/\nu$, Reynolds number based on momentum loss thickness; $Re_D = Du_\tau/\nu$, Reynolds number based on the friction velocity and the Pitot tube outside diameter D; $Re_y = yu_\tau/\nu$, Reynolds number based on the friction velocity u_τ and distance y of the tube axis from the wall; d, Pitot tube inside diameter; ε, displacement of the effective pitot tube center relative to the geometric tube axis; α, transverse velocity gradient parameter over the height of the Pitot tube entrance aperture; y', current y distance from the tube geometric axis.

LITERATURE CITED

1. N. P. Mikhailova and E. U. Repik, "Influence of viscosity on readings of a Pitot tube at low flow velocities," Izv. Akad. Nauk SSSR, Mekh. Zhidk. Gaza, No. 1, 136-139 (1976).
2. N. P. Mikhailova and E. U. Repik, "Influence of viscosity on the readings of two-dimensional micropitot tubes at low flow velocities," Izv. Akad. Nauk SSSR, Mekh. Zhidk. Gaza, No. 6, 148-152 (1979).
3. J. M. Hall, "The displacement effect of a sphere in a two-dimensional shear flow," J. Fluid Mech., 1, Pt. 2, 142-162 (1956).
4. M. J. Lighthill, "Contribution to the theory of the Pitot tube displacement effect," J. Fluid Mech., 2, Pt. 5, 493-512 (1957).
5. P. O. A. L. Davies, "The behavior of a Pitot tube in transverse shear," J. Fluid Mech., 3, Pt. 5, 441-456 (1958).
6. F. A. MacMillan, "Experiments on Pitot tubes in shear flow," ARC RM N 3028 (1956).
7. E. U. Repik, "Measurement of velocity in a boundary layer with the aid of a Pitot tube," Inzh.-Fiz. Zh., 22, No. 3, 505-510 (1972).
8. D. B. Spalding, "A single formula for the 'Law of the wall'," J. Appl. Mech., 28, No. 3, 455-458 (1961).
9. H. Reichardt, "Vollständige Darstellung der turbulenten Geschwindigkeitsverteilung in glatten Leitungen," Z. angew. Math. Mech., vol. 31, 208-219 (1951).
10. J. H. Preston, "The determination of turbulent skin friction by means of Pitot tubes," J. R. Aeron. Soc., 58, No. 158, 109-121 (1964).
11. V. C. Patel, "Calibration of the Preston tube and limitations on its use in pressure gradients," J. Fluid Mech., 23, Pt. 1, 185-208 (1965).
12. V. K. Kuzenkov, N. P. Mikhailova, and E. U. Repik, "An experimental determination of the resistance profile by the momentum method," Uchen. Zap. Tsentr. Aero. Gidro. Inst., 15, No. 1, 110-114 (1984).
13. S. H. Chue, "Pressure probes for fluid measurements," Prog. Aerospace Sci., 16, No. 2, 147-223 (1975).

CHARACTERISTICS OF A PLANE TURBULENT JET IN A BOUNDED DRIFTING FLOW

S. K. Voronov, T. A. Girshovich, and A. N. Grishin

UDC 532.525.2

A method is proposed for computing the characteristics of a plane turbulent jet escaping at a right angle to a flow constrained by channel walls. Results are presented of an experimental investigation of such jets and their comparison with design data.

A large number of papers is devoted to the theoretical and experimental investigation of jets in drifting flow. However, a systematic experimental investigation of the influence of the boundedness of the flow on the plane jet propagation characteristics has, visibly, not been performed. In the known papers [1-3] the investigations were carried out just in channels with specific geometry and, consequently, mainly just the jet trajectories were determined in the experiment. A theoretical solution of the problem of determining the characteristics of plane turbulent jets escaping at an angle to the flow constrained by channel walls does not exist in the literature, insofar as we know.

A method is proposed below for the computation of such jets on the basis of the solutions of problems on a plane jet in an unbounded drifting flow [4-7] and on the rarefaction in the reverse flow zone behind a plane jet in a constrained drifting flow [8]. Moreover, results of an experimental investigation of the influence of structural and dynamical parameters on characteristics of a plane jet are elucidated.

Sergo Ordzhonikidze Moscow Aviation Institute. Translated from Inzhenerno-Fizicheskii Zhurnal, Vol. 48, No. 6, pp. 904-911, June, 1985. Original article submitted April 16, 1984.

0022-0841/85/4806-0649$09.50